5. Numerical simulation of interaction between internal solitary waves and submerged ridges / Zhu H., Wang L., Avital E. J., Tang H., Williams J. J. R. // Applied Ocean Research. 2016. Vol. 58. P. 118–134. doi: 10.1016/j.apor.2016.03.017
6. Smith S., Crockett J. Experiments on nonlinear harmonic wave generation from colliding internal wave beams // Experimental Thermal and Fluid Science. 2014. Vol. 54. P. 93–101. doi: 10.1016/j.expthermflusci.2014.01.012
7. Massel S. R. On the nonlinear internal waves propagating in an inhomogeneous shallow sea // Oceanologia. 2016. Vol. 58, Issue 2. P. 59–70. doi: 10.1016/j.oceano.2016.01.005
8. Avramenko O. V., Naradovyi V. V., Selezov I. T. Energy of Motion of Internal and Surface Waves in a Two-Layer Hydrodynamic System // Journal of Mathematical Sciences. 2018. Vol. 229, Issue 3. P. 241–252. doi: 10.1007/s10958-018-3674-7
9. Avramenko O., Lunyova M., Naradovyi V. Wave propagation in a three-layer semi-infinite hydrodynamic system with a rigid lid // Eastern-European Journal of Enterprise Technologies. 2017. Vol. 5, Issue 5 (89). P. 58–66. doi: 10.15587/1729-4061.2017.111941
10. Nayfeh A. H. Nonlinear Propagation of Wave-Packets on Fluid Interfaces // Journal of Applied Mechanics. 1976. Vol. 43, Issue 4. P. 584. doi: 10.1115/1.3423936
11. Tarapov I. E. Continuum Mechanics. Vol. 3. Mechanics of Inviscid Liquid. Kharkiv: Zolotye Stranitsy, 2005.
12. Avramenko O. V., Hurtovyi Yu. V., Naradovyi V. V. Analiz enerhiyi khvylovoho rukhu v dvosharovykh hidrodynamichnykh systemakh // Naukovi zapysky. Seriya: Matematychni nauky. 2014. Issue 73. P. 3–8.

Досліджено метод оцінки атмосферної турбулентності за статистичними характеристиками обвідної сигналів содара. Показано, що обвідна ехо-сигналів розподілена по закону Райса, параметр закону розподілу пов'язаний з інтенсивністю турбулентності. Отримані значення параметра закону розподілу ехосигналів для турбулентності певних класів. Використання дослідженого методу додатково до вже застосованих дозволить збільшити точність і часове розрізнення содарів

Ключові слова: акустичне зондування, содар, турбулентність, ехо-сигнал, обвідна, авіаційна метеорологія, вітрова енергетика

Исследован метод оценки атмосферной турбулентности по статистическим характеристикам огибающей сигналов содара. Показано, что огибающая эхо-сигналов распределена по закону Райса, параметр закона распределения связан с интенсивностью турбулентности. Получены значения параметра закона распределения эхо-сигналов для турбулентности определённых классов. Использование исследованного метода дополнительно к уже применяемым позволит увеличить точность и временное разрешение содаров

Ключевые слова: акустическое зондирование, содар, турбулентность, эхо-сигнал, огибающая, авиационная метеорология, ветровая энергетика

UDC 551.501.7

DOI: 10.15587/1729-4061.2018.127699

STUDY OF THE METHOD FOR ASSESSING ATMOSPHERIC TURBULENCE BY THE ENVELOPE OF SODAR SIGNALS

S. Sheiko
PhD
Department of Media Engineering and Information Radio Electronic Systems
Kharkiv National University of Radio Electronics
Nauky ave., 14, Kharkiv, Ukraine, 61166
E-mail: sergiy.sheiko@nure.ua

1. Introduction

Acoustic locators (sodars) are important sources of information about velocity, wind direction and the degree of turbulence of air masses at altitudes of up to 1 km. Information of sodars is widely used for studies of the atmosphere [1–3], local and global weather forecasts [4, 5], air traffic control services [1, 6], for monitoring the atmosphere at wind farms [7–10], near potential sources of hazardous emissions [1], etc.

As a rule, monostatic three-beam sodars with one vertical beam and two beams, deviated from the vertical by 20...30° in mutually perpendicular directions are used [1, 2, 5–10]. The range to scattering volume is determined by the time of an echo signal delay, and wind projection onto the direction of sounding is determined by the Doppler frequency shift. Turbulence intensity is estimated by the power of a return signal and the width of the Doppler spectrum. The general tendency of sodars improvement is to increase reliability and operative measurements [1–10]. This is especially important when detecting hazardous meteorological phenomena, for example, in the aircraft takeoff-landing area [6]. Taking into consideration the increasing requirements for measurement accuracy and temporal resolution of sodars, the relevant task is to improve the methods for obtaining meteorological information from parameters of echo signals.

2. Literature review and problem statement

Analysis of up-to-date works on acoustic sounding of the atmosphere shows that the efforts of many researchers are directed to development of the methods for obtaining meteorological information form echo-signals.

Turbulence intensity is usually assessed by power of return signal and by the width of the Doppler spectrum [1, 11]. Some methods for turbulence measuring are based on empirical formulas that describe the relationship between power of signals and coefficients of structural functions of temperature field and wind velocity [3, 11, 12]. The width of the Doppler frequency spectrum that is related to the root mean square deviation of velocities in scattering volume is measured in other methods [11, 13, 14].

A common drawback of all methods for turbulence measuring is the fact that it is possible to obtain reliable results only on long intervals of measurements. In paper [11], averaging of measurement results within 10 min was used in order to obtain vertical profiles of structural functions of temperature fields and wind velocity. In the experiments, described in article [12], the signals of eight microphones also on the interval of more than 10 min were averaged in order to obtain vertical profiles of echo signals power, while for the data, obtained from the meteorological mast, average time of less than 5 min was enough. The study of the influence of time of averaging on the quality of measurement of turbulence characteristics in papers [13, 14] shows that averaging signals, their spectra or results of single measurements within the time from 10 min to 1 hour is required. This is due to the random nature of acoustic echo-signals, as well as the final signal-to-noise ratio.

Signal-to-noise ratio is limited, on the one hand, by the energy potential of the system. Output acoustic power of sodars does not exceed 300 W, which is caused by non-linear interaction of sound and atmospheric air [15]. On the other hand, sodars often operate under conditions of a high level of external acoustic interference, especially in the airport zones [6] or in industrial areas [12]. Special aerials, based on phased aerial arrays, are developed for improvement of power efficiency of sodars and their protection from external interference [15, 16]. These measures increase measurement reliability, but do not significantly decrease the time of measurements.

Measurements on several frequencies using pulse [17] or continuous [18] signal are applied in a number of cases for an increase in the time resolution of a sodar. Results of measurements at a given range are averaged by the frequencies ensemble. The use of some frequencies decreases the minimally permissible signal-to-noise ratio compared to signal-frequency sounding. In addition, accuracy of measurement of meteorological parameters within a short time improves. One of the drawbacks of the multi-frequency method is a decrease in effectiveness of an acoustic aerial when setting its optimal frequency.

In the patent [19], an alternative method of determining turbulence parameters by statistical characteristics of the envelope of sodar signals was proposed. The method does not require measurement of the Doppler spectrum and makes it possible to refer turbulence to a particular class according to the degree of its intensity. Experimental turbulence measurements with the help of this method have not been performed so far.

In the case of a positive result of research, implementation of this method in sodar signal processing will allow us to use the information of echo-signals more fully, to improve temporal resolution and accuracy of determining turbulence parameters.

3. The aim and objectives of the study

The aim of present study is to theoretically substantiate and experimentally determine the possibilities of the method for turbulence intensity measurement by the envelope of sodar signals.

To accomplish the aim, the following tasks have been set:

– to carry out theoretical analysis of the relation of statistical characteristics of the envelope of acoustic echo-signals to intensity of atmospheric turbulence;

– to apply the method of turbulence intensity measurement using characteristics of the envelope of acoustic echo-signals when processing sodar signal records;

– to explore convergence of the experimental law of distribution of the envelope of acoustic echo-signals to the theoretical law at different measurement time;

– to establish the possibility of turbulence classification by the envelope using the records of acoustic echo-signals, obtained under different meteorological conditions.

4. Theoretical analysis of statistical characteristics of the envelope of acoustic echo-signals

During acoustic probing of the atmosphere within the scattering volume, there are many elementary scatters, the number, dimensions and location of which are random. In this case, a number of scattered signals arrive at that reception point, and the envelope of the total scattered input signal E should be considered as a random magnitude, changing in time. Depending on the state of scattering medium, the total input signal E obeys a rather determined distribution law. Knowing this law and its parameters, it is possible to determine the state of the atmosphere, specifically turbulence intensity.

In the boundary layer of the air, fragmentation of turbulent vortices goes on until the magnitude of Reynolds number that is less than the critical value is achieved [1]. The emerging smallest perturbations, the size of which corresponds to the inner turbulence scale are resistant. Strong reflected acoustic signals occur at large enough spectral density of temperature fluctuations, the scale of which is equal to half the length of the emitting sound wave [1].

Since temperature pulsations and wind pulsations are correlated, the reflected acoustic signal carries information about atmospheric turbulence, the intensity of which can be determined from the measured characteristics of this signal. In this case, large-scale turbulence causes only additional shift of the entire spectrum of the Doppler frequencies of the scattered signal by the frequency axis. Small-scale vortices and thermal pulsations, which are commensurate with dimensions of scattering volume and the wavelength of the acoustic locator, cause fluctuations of the envelope of the signal and expansion of its range.

The instantaneous value of the input signal of the acoustic locator [1]

$$e(t) = E_0 \cos(\omega t - \phi) + \sum_{i=1}^{n} E_i \cos(\omega t - \phi_i), \quad (1)$$

where E_0, E_i are the amplitudes of the regular and random components of the input signal; ϕ, ϕ_i are the phases of the regular and random components of the input signal.

Since phase of the regular component at the reception point is constant, for further transformation we will put $\phi=0$. If the resulting amplitude of the sum of random components is designated as E_Σ, and the phase is designated as ϕ_Σ, expression (1) will take the form:

$$e(t) = E_0 \cos\omega t + E_\Sigma \cos(\omega t - \phi_\Sigma). \quad (2)$$

Since scattered waves are added together at the reception point with random relative phases, evenly distributed in the interval $0...2\pi$, amplitude E_Σ of the total scattered signal is random and phase ϕ_Σ is evenly distributed with density $1/2\pi$.

Analysis of the amplitude of the resulting signal can be performed according to the known technique, applied when considering narrowband random processes, reflected radar signals, signals in tropospheric and ionospheric communications lines.

Let us decompose fluctuation

$$e_\Sigma(t) = E_\Sigma \cos(\omega t - \phi_\Sigma)$$

into two orthogonal components, of which the cosine component coincides by phase with the direct wave field:

$$e_\Sigma(t) = E_{\Sigma 1} \cos\omega t + E_{\Sigma 2} \cos\omega t, \quad (3)$$

where

$$E_{\Sigma 1} = \sum_{i=1}^{n} E_i \cos\phi_i; \quad E_{\Sigma 2} = \sum_{i=1}^{n} E_i \sin\phi_i;$$

$$E_\Sigma = \sqrt{E_{\Sigma 1}^2 + E_{\Sigma 2}^2}; \quad tg\phi_\Sigma = \frac{E_{\Sigma 2}}{E_{\Sigma 1}}.$$

Representing fluctuations with amplitudes E_0, $E_{\Sigma 1}$, $E_{\Sigma 2}$ with the help of vectors, we will write down:

$$\vec{E}_1 = \vec{E}_0 + \vec{E}_{\Sigma 1}; \quad \vec{E}_2 = \vec{E}_{\Sigma 2}. \quad (4)$$

Vectors $\vec{E}_1$ and $\vec{E}_2$ are orthogonal and amplitudes of orthogonal components E_1 and E_2 are independent magnitudes. Let us find the law of probability distribution E.

At successive atmosphere soundings, the number of elementary scatters in volume n, differences of distances to them Δr_i, coefficient of reflection from each lens R_i will change due to a change in their dimensions and so on. Therefore, amplitudes of orthogonal components $E_{\Sigma 1}$ and $E_{\Sigma 2}$ will change.

Let us assume the following: the number of scattered signals is large enough, amplitudes of particular scattered components are much smaller than the resulting amplitude, phases of particular components E_i are distributed arbitrarily; resulting power of echo-signals over observation time is constant.

For the sums with the specified properties, the central limit theorem of probability theory is true, that is why we can consider that random magnitudes E_1 and E_2 of the orthogonal components are distributed by the normal law. Mathematical expectations of these components: $\overline{E}_1 = \overline{E}_0$; $\overline{E}_2 = 0$. Given the symmetry of decomposition of a random resulting received signal to orthogonal components, it can be argued that dispersions of amplitudes of the orthogonal components are

$$\sigma_1^2 = \sigma_2^2 = \sigma^2 = \sum_{i=1}^{n} E_i^2 / 2. \quad (5)$$

Orthogonal components are statistically independent. That is why two-dimensional density of probability of random magnitudes E_1 and E_2 is equal to the product of

$$p(E_1, E_2) = p(E_1) \cdot p(E_2) = \\ = \frac{1}{2\pi\sigma^2} \exp\left(-\frac{(E_1 - E_0)^2 + E_2^2}{2\sigma^2} \right). \quad (6)$$

We will find one-dimensional law of distribution of the resulting envelope of echo-signal E. Probability of finding resulting magnitude E within elementary rectangle $dE_1 \times dE_2$ is equal to

$$p(E_1, E_2) dE_1 dE_2 = p(E_1) p(E_2) dE_1 dE_2. \quad (7)$$

Amplitude E and phase ϕ of the resulting echo-signal are random coordinates of the point in coordinate system E_1, E_2, where $E_1 = E \times \cos\phi$, $E_2 = E \times \sin\phi$. Turning to new variables from formula

$$p(E, \phi) = p(E\cos\phi, E\sin\phi) \cdot |D|, \quad (8)$$

we will obtain joint density of probabilities for random magnitudes E and ϕ:

$$p(E, \phi) = \frac{E}{2\pi\sigma^2} \exp\left(-\frac{E^2 + E_0^2 - 2E_0 E\cos\phi}{2\sigma^2} \right). \quad (9)$$

Integrating (9) on all possible values of ϕ, we find one-dimensional probability density for E:

$$p(E) = \int_0^{2\pi} p(E, \phi) d\phi = \frac{E}{\sigma^2} \exp\left(-\frac{E^2 + E_0^2}{2\sigma^2} \right) I_0\left(\frac{E_0 E}{\sigma^2} \right), \quad (10)$$

where I_0 is the modified zero-order Bessel function of the first kind.

Expression (10) of probability density of the envelope of acoustic echo-signals is a generalized Rayleigh law (the Rice law). Parameter of the generalized Rayleigh law, characterizing the processes of formation of a resultant signal, is magnitude $k = E_0/\sigma_E$. If there is a stable stratification in the scattering volume, the regular component increases and the sum of scattered components of the reflected signal decreases, as a result, parameter k increases. At destruction of stratification and an increase in turbulence, the regular component and magnitude k decreases abruptly, tending in the limit to zero.

Let us determine dependence k on parameters of envelope E of an echo-signal.

$$\overline{E^2} = \int_0^{\infty} p(E) E^2 dE = \\ = \int_0^{\infty} E^2 \frac{E}{\sigma^2} \exp\left(-\frac{E^2 + E_0^2}{2\sigma^2} \right) I_0\left(\frac{E_0 E}{\sigma^2} \right) dE = 2\sigma^2(1 + k^2). \quad (11)$$

$$\overline{E} = \int_0^\infty E \frac{E}{\sigma^2} \exp\left(-\frac{E^2+E_0^2}{2\sigma^2}\right) I_0\left(\frac{E_0 E}{\sigma^2}\right) dE =$$
$$= \sqrt{\frac{\pi}{2}}\sigma \exp\left(-\frac{k}{2}\right)\left[(1+k^2) I_0\left(\frac{k^2}{2}\right) + k^2 I_1\left(\frac{k^2}{2}\right)\right]. \quad (12)$$

where I_0 and I_1 are the modified zero-order Bessel function of the first kind. From formulas (11) and (12), it is possible to find the relationship

$$\frac{\overline{E^2}}{\overline{E}^2} = \frac{4}{\pi} \cdot \frac{(1+k^2)\cdot \exp(k^2/2)}{\left[(1+k^2)\cdot I_0(k^2/2) + k^2 \cdot I_1(k^2/2)\right]^2}. \quad (13)$$

Calculation results from formula (13) are represented in the form of the diagram in Fig. 1, where parameter k is represented in more convenient form K=20lg(k) in order to decrease the dynamic range of this parameter.

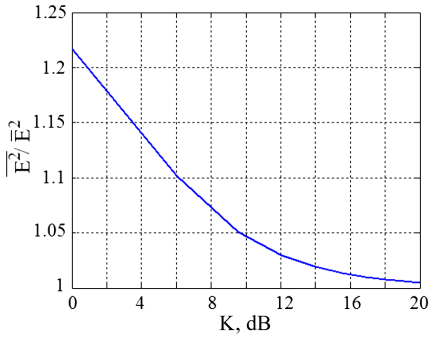

Fig. 1. Dependence of ratio $\overline{E^2}/\overline{E}^2$ on parameter K

By degree of impact of aircraft, atmospheric turbulence is divided into four classes and can be quantitatively described by root mean square values of pulsations of the vertical component of wind velocity. According to ICAO criteria, turbulence is classified by intensity as weak, moderate, strong and storm [20]. Table 1 shows the magnitudes of root mean square pulsations of vertical wind, corresponding to this classification, and corresponding values of parameter K at standard atmospheric stratification [19].

Table 1

Criteria of turbulence intensity division into classes

Turbulence intensity	Root mean square value of wind pulsations, σ_W, m/s	K, dB
Weak	$\sigma_W \leq 0.5$	$K \geq 16$
Moderate	$0.5 < \sigma_W \leq 2.5$	$16 > K \geq 8$
Strong	$2.5 < \sigma_W \leq 4.0$	$8 > K \geq 0$
Storm	$\sigma_W > 4.0$	$K < 0$

Thus, it is possible to assess atmospheric turbulence intensity by applying the following algorithm of sodar signals processing:

– registration of echo-signals envelope E of within some observation time T_H;

– calculation of ratio $\overline{E^2}/\overline{E}^2$ for measured implementation of envelope E;

– determining the value of parameter K in accordance with expression (13) and data from the diagram in Fig. 1;

– classification of turbulence in accordance with the data from Table 1.

5. Experimental results of turbulence classification by the characteristics of the envelope of acoustic echo-signals

The data, obtained by the sodar at Kharkiv National University of Radio Electronics, were used in the study. A large amount of experimental data in the form of digital records of echo-signals was obtained at this sodar in the summer in 2011 and 2012 [21, 22]. In the summertime, warming of the underlying surface, which is accompanied by intense turbulent exchange, is distinctly pronounced. Therefore, the selected records are well suited for measuring turbulence.

In the described experiments sounding was performed vertically. Sodar parameters: frequency of probing signal is 5 kHz, electric power of the transmitter is 160 W, duration of sounding pulse is 3 ms, pulse repetition period is 1 s, duration of implementations is 1 hour, transmitting aerial is the phased array of loudspeakers 4×4, parabolic-reflector receiving aerial of 0,8 m in diameter.

The records of echo-signals are represented in the form of 2-dimensional arrays of amplitude $E(i, j)$. Columns of array $E_i(j)$ are single vertical profiles of echo-signals, and each line of array $E_j(i)$ is a series of discrete readings of echo-signals for altitude $h=\Delta h \times j$, where Δh=0,5 m is the discrete altitude pitch.

The obtained original material was classified by the authors of papers [21, 22] and selected according to the principle of conformity of echo-signals: to a fluctuating ground level, a perturbed layer, a completely perturbed ground layer. These records were obtained as the underlying surface was warmed and correspond to an increase in intensity of turbulent exchange. In all cases, horizontal wind velocity is close to zero, it is clear without any cumulonimbus cloud. Fig. 2 in the form of a halftone image gives an example of altitude-temporal implementation of the amplitude of acoustic echo-signals, obtained under conditions of intense solar warmup of the underlying surface, and Fig. 3 shows a fragment of the envelope of echo-signals from the altitude h=30 m.

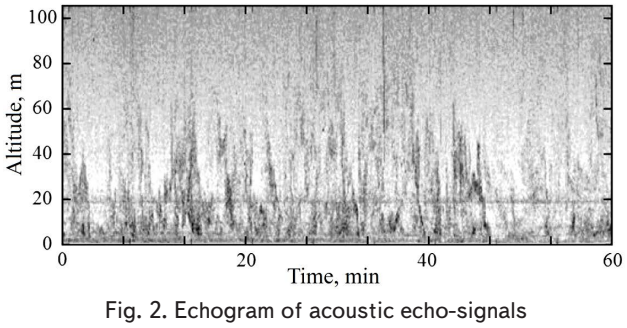

Fig. 2. Echogram of acoustic echo-signals

Convergence of the experimental law of distribution of envelope E of echo-signals to theoretical distribution (10) depends on observation time T_o. Original assessment of parameters of the distribution law was performed by the moments method. Sample mathematic expectation M_E and dispersion D_E were calculated:

$$M_E = (1/n)\cdot \sum_{i=1}^{n} E_j(i),$$

$$D_E = (1/n)\cdot\sum_{i=1}^{n}(E_j(i)-M_E)^2, \quad (14)$$

where number of samples n depends on observation time, $n=T_o/T$. To obtain minimally shifted estimates of distribution parameters $\tilde{E}_0$ and $\tilde{\sigma}$, their values were sought for in the vicinity of M_E and $\sqrt{D_E}$ until obtaining the minimum of disagreement measure.

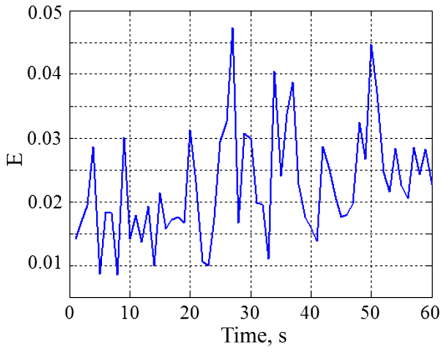

Fig. 3. A fragment of envelope E of echo-signals from altitude of 30 m

Fig. 4 shows experimental distributions of probability p of envelope E of acoustic echo-signals and their approximation by the Race distribution (10) for observation intervals of 5 min (Fig. 4, *a*), 10 min (Fig. 4, *b*), 20 min. (Fig. 4, *c*) and 40 min (Fig. 4, *d*).

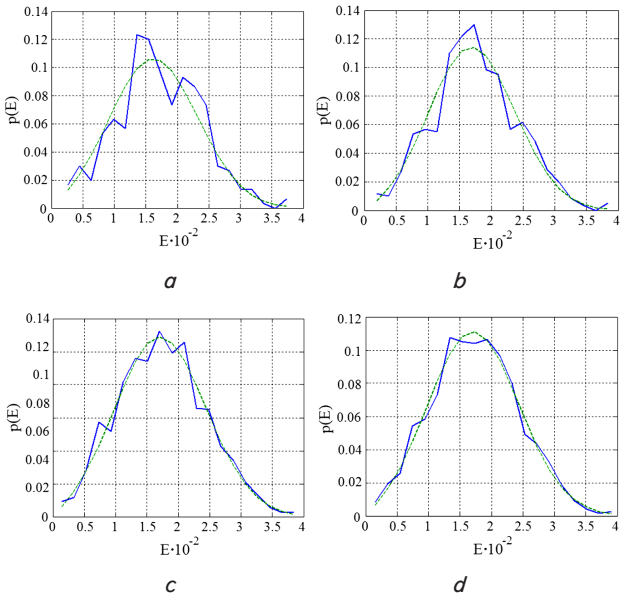

Fig. 4. Experimental distributions of probability p of envelope E of acoustic echo-signals (blue continuous line) and their approximation by the Rice distribution (green dash line) for observation intervals: *a* – 5 min, *b* – 10 min, *c* – 20 min, *d* – 40 min

Echo-signals meet the condition of strongly perturbed ground layer at altitude h=15 m. To reduce the influence of pulsed acoustic interference that existed in the recording, readings of amplitudes of echo-signals with magnitude $E>5M_E$ were not included in statistics. Less than 10 samples were practically discarded from implementation of 1 hour of duration. Visually, the law of distribution of envelope (E) well agrees with the Rice law at observation time T_o>5 min.

As a measure of misalignment of the distribution laws, we used the Pearson criterion [23], in which magnitude

$$\chi^2 = n\sum_{x=1}^{m}\frac{(p_x - v_x)^2}{p_x}, \quad (15)$$

was accepted as a relative measure of divergence of theoretical p and experimental v distributions, where m is the number of intervals of grouping of observation results, at m=20; there is the best qualitative correspondence of theoretical and experimental distributions; $v_x=n_x/n$, n_x is the number of samples in the interval of grouping with number x. The hypothesis that laws of distribution of p and v do not agree is true with probability

$$P_{\chi^2} = \int_{\chi^2}^{\infty} p_{\chi^2}(a)\mathrm{d}a, \quad (16)$$

where

$$p_{\chi^2}(a) = \frac{1}{2\Gamma(m/2)}\cdot(a/2)^{(m/2)-1}\exp(-a/2)$$

is the law of probability distribution, $\Gamma(m/2)$ is the gamma-function.

Fig. 5 shows experimental dependences of magnitude P_{χ^2} on duration of observation interval at sounding altitudes of 15 m (Fig. 5, *a*), 30 m (Fig. 5, *b*) and 45 m (Fig. 5, *c*), respectively.

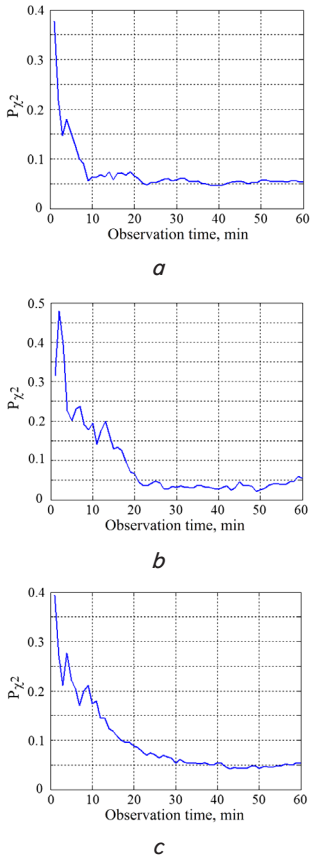

Fig. 5. Experimental dependences of magnitude P_{χ^2} on duration of observation interval T_o at sounding altitudes: *a* – 15 m, *b* – 30 m, *c* – 45 m

Analysis of a large number of similar dependencies for records available, showed that on the samples of duration of more than 30 min (1,800 readings), magnitude $P_{\chi^2} \approx 5\ \%$ does not decrease at an increase in observation time.

More rapid convergence of the law of echo-signals distribution to the Rice law (about 10 minutes) is observed in an envelope of echo-signals from low altitudes (approximately up to 20 m). This, apparently, can be explained by large signal-to-noise ratio at low altitudes of sounding.

To assess the possibility of classification of atmospheric turbulence by the parameters of the envelope of acoustic echo-signals, the dependence of relation $\overline{E^2}/\overline{E}^2$ on duration of the observation interval was studied.

Experimental dependences $\overline{E^2}/\overline{E}^2$ and $\overline{E^2}$ on T_o for a fluctuating layer (Fig. 6), a perturbed layer (Fig. 7) and a completely perturbed atmospheric layer (Fig. 8) are shown below. These states correspond to gradual warming of the underlying surface and an increase in intensity of turbulent exchange. Magnitude $\overline{E^2}$ corresponds to average power of received echo-signals, traditionally measured in acoustic locators to assess turbulence intensity.

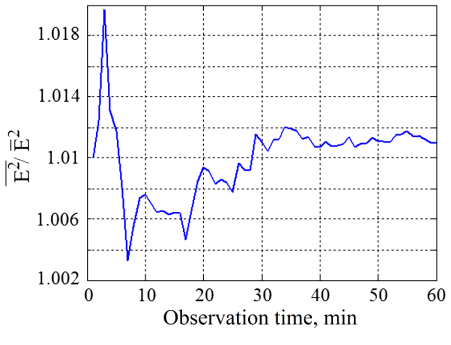

a

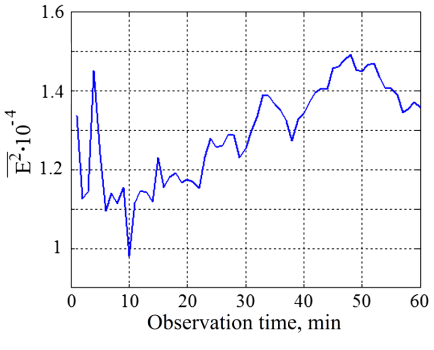

b

Fig. 6. Experimental dependences $\overline{E^2}/\overline{E}^2$ and $\overline{E^2}$ on observation time T_o for a fluctuating layer: *a* – dependence $\overline{E^2}/\overline{E}^2(T_o)$, *b* – dependence $\overline{E^2}(T_o)$

As an analysis of these and other similar dependences, obtained in the studies, shows, estimation magnitude $\overline{E^2}/\overline{E}^2$ changes little already at the observation interval of more than 10...30 minutes. An interesting feature is the fact that, 10 minutes of observation time is enough in the case of sounding more perturbed medium and 20 min and more – for less perturbed medium. It is also important to note that magnitude $\overline{E^2}/\overline{E}^2$ often converge to a stationary value at less monitoring time T_o, than magnitude $\overline{E^2}$.

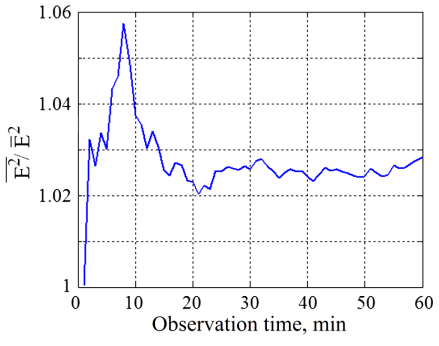

a

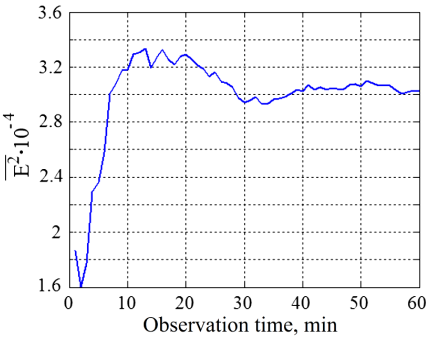

b

Fig. 7. Experimental dependences $\overline{E^2}/\overline{E}^2$ and $\overline{E^2}$ on observation time T_o for a perturbed layer: *a* – dependence $\overline{E^2}/\overline{E}^2(T_o)$, *b* – dependence $\overline{E^2}(T_o)$

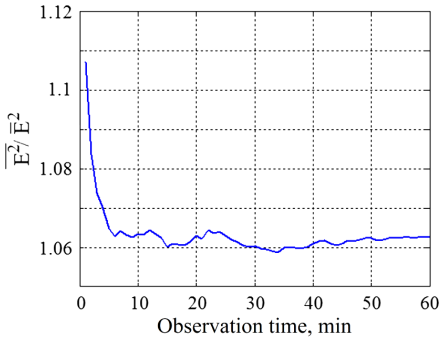

a

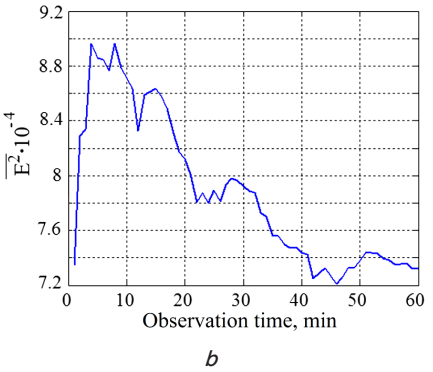

b

Fig. 8. Experimental dependences $\overline{E^2}/\overline{E}^2$ and $\overline{E^2}$ on observation time T_o for a completely perturbed layer: *a* – dependence $\overline{E^2}/\overline{E}^2(T_o)$, *b* – dependence $\overline{E^2}(T_o)$

Table 2 shows the results of assessment of statistical characteristics of the envelope and turbulence classification according to Table 1.

Table 2

Statistical characteristics of the envelope and turbulence classification

Type of echo-signal	$\overline{E^2}/\overline{E}^2$	k	K, dB	Turbulence class according to Table 1
Fluctuating layer	1.012	7.16	17.1	Weak
Perturbed layer	1.025	4.73	13.5	Moderate
Completely perturbed layer	1.061	2.92	9.3	Moderate

Estimates, given in Table 2, prove that ratio $\overline{E^2}/\overline{E}^2$, as well as parameters k and K, calculated from it, can be used as indicators of intensity of atmospheric turbulence. By a change in these parameters, an increase in turbulent exchange intensity at gradual heating of the underlying surface in the original experiment is confidently traced.

6. Discussion of the results of research and their application in acoustic sounding of the atmosphere

In this paper, the theoretical analysis and experimental study of method for assessing atmospheric turbulence by statistical characteristics of the envelope of a sodar signal, proposed in patent [19], were performed.

According to performed theoretical analysis, it is sufficient to calculate the ratio of average power to power of average $\overline{E^2}/\overline{E}^2$. in order to evaluate turbulence by the echo-signal envelope E.

To process experimental records of acoustic echo-signals, only general meteorological conditions, in which they were obtained, were known. Specifically: date, current time, ground surface air temperature, air humidity, and average wind velocity. It follows from these data that the records were obtained as the underlying surface warmed and correspond to an increase in intensity of turbulent exchange. This assumption was the basis for numerical assessment of turbulence intensity.

The drawback of the applied approach is that true values of turbulence degree in this study were not known. Therefore, it will be subsequently required to perform additional acoustic and contact measurements to design accurate criteria for turbulence classification by ratio $\overline{E^2}/\overline{E}^2$. Moreover, it is necessary to have true values of coefficients of structural functions of temperature field and wind velocity for correct comparison. The noticeable difficulty for performing simultaneous acoustic and contact measurements is the need for the use of a meteorological mast.

For the same reason, convergence of measured values $\overline{E^2}/\overline{E}^2$ and $\overline{E^2}$ not to the true value but to the stationary value was studied. Estimate of ratio $\overline{E^2}/\overline{E}^2$ changes little at observation interval of more than 10...30 minutes. 10 min of observation time is enough in the case of sounding a more perturbed medium and 20 min and more – for little perturbed medium.

In most studied records, magnitude $\overline{E^2}/\overline{E}^2$ converges to a stationary value at less observation time than average power $\overline{E^2}$. This can be explained by synchronicity fluctuations of estimates $\overline{E^2}$ and $\overline{E}^2$ at different observation time.

When sounding the medium with intense turbulence, ratio $\overline{E^2}/\overline{E}^2$ converges to a stationary value by up to 2...3 times faster than average power $\overline{E^2}$, which suggests a possibility of much faster detection of strong turbulence. This is especially important for detecting dangerous meteorological phenomena in the takeoff and landing zones.

Introduction of the studied method in processing sodar data does not require any changes in the hardware. This will make it possible to use more fully the information of echo-signals without considerable material expenses, to improve temporal resolution and accuracy of determining turbulence parameters.

Restrictions on the use of the studied method do not differ from those that are common to all sodars, specifically: the influence of precipitation, acoustic interference, limitation of the maximum altitude of sounding by strong wind and temperature inversion.

7. Conclusions

1. Theoretical analysis showed that the envelope of sodar echo-signals is distributed by the Rice law. The parameter of the distribution law is unambiguously associated with intensity of atmospheric turbulence.

2. Assuming standard stratification of atmosphere, the values of the parameter of the law of envelope distribution for four classes of atmospheric turbulence according to the ICAO classification were calculated: weak, moderate, strong, and stormy.

3. Numerical assessment showed that the theoretical and experimental laws of distribution of the envelope of sodar signals mismatch with probability of less than 5 % at measurement time from 10 to 30 minutes. More rapid convergence of the law of echo-signal distribution to the Rice law (about 10 minutes) is observed at low altitudes of sounding (up to 20 m). This can be explained by the large signal-to-noise ratio.

4. The possibility of classification of atmospheric turbulence by ratio $\overline{E^2}/\overline{E}^2$ to the measured echo-signal envelope E was shown experimentally. It was established that ratio $\overline{E^2}/\overline{E}^2$ almost does not change at the observation interval of more than 10...30 minutes. Moreover, the higher the turbulence intensity, the faster the measurement results converge to a stationary value. This indicates the possibility of a more rapid detection of zones with high turbulence intensity compared with the sodars, recording only average power of a signal.

5. Consideration of statistical characteristics of the envelope of a sodar signal as a complement to already used methods for turbulence determining makes it possible to decrease the time and increase accuracy of measurement. In this case, it is not required to make any changes to sodar hardware.

Acknowledgement

The author expresses his sincere appreciation to the authors of papers [21, 22] V. I. Leonidov and. V. V. Semenets for the provided records of acoustic echo-signals and useful discussions.

References

1. Krasnenko N. P. Akusticheskoe zondirovanie atmosfernogo pogranichnogo sloya. Tomsk: Vodoley, 2001. 278 p.
2. A Comparison of Vertical Atmospheric Wind Profiles Obtained from Monostatic Sodar and Unmanned Aerial Vehicle-Based Acoustic Tomography / Finn A., Rogers K., Rice F., Meade J., Holland G., May P. // Journal of Atmospheric and Oceanic Technology. 2017. Vol. 34, Issue 10. P. 2311–2328. doi: 10.1175/jtech-d-17-0070.1
3. Kouznetsov R. D. Quantitative estimate of the role of temperature gradients in sodar echo signal formation // IOP Conference Series: Earth and Environmental Science. 2008. Vol. 1. P. 012039. doi: 10.1088/1755-1307/1/1/012039
4. LACOST, an atmospheric laboratory on the Tyrrhenian coastline / Argentini S., Petenko I., Bucci S., Mastrantonio G., Conidi A., Federico S. et. al. // 18th International Symposium for the Advancement of Boundary layer remote Sensing. Varna, 2016. URL: https://www.researchgate.net/publication/322069919
5. Comparison studies of sodar winds with the NCEP/NCAR Reanalysis II winds over a semi-arid region Anantapur / Reddy T. L., Reddy N. S. K., Gopal K. R., Balakrishnaiah G., Reddy R. R. // International Tropical Meteorology Symposium. Ahmedabad, 2017. P. 10–13. URL: https://www.researchgate.net/publication/322024402
6. Conceptual model for runway change procedure in Guarulhos International Airport based on SODAR data / Luiz Silva W., Albuquerque Neto F. L., França G. B., Matschinske M. R. // The Aeronautical Journal. 2016. Vol. 120, Issue 1227. P. 725–734. doi: 10.1017/aer.2016.33
7. Remote Sensing for Wind Energy / Peña A., Hasager C. B., Lange J. et. al. // DTU Wind Energy. 2013. 308 p. URL: http://orbit.dtu.dk/files/55501125/Remote_Sensing_for_Wind_Energy.pdf
8. Chaurasiya P. K., Ahmed S., Warudkar V. Wind characteristics observation using Doppler-SODAR for wind energy applications // Resource-Efficient Technologies. 2017. Vol. 3, Issue 4. P. 495–505. doi: 10.1016/j.reffit.2017.07.001
9. Khan K. S., Tariq M. Wind resource assessment using SODAR and meteorological mast – A case study of Pakistan // Renewable and Sustainable Energy Reviews. 2018. Vol. 81. P. 2443–2449. doi: 10.1016/j.rser.2017.06.050
10. Yazidi H. Sodar measurements in wind energy industry state of the art. URL: https://www.academia.edu/20671917
11. Krasnenko N. P., Shamanaeva L. G. Sodars and their application for investigation of the turbulent structure of the lower atmosphere // IOP Conference Series: Earth and Environmental Science. 2016. Vol. 48. P. 012025. doi: 10.1088/1755-1315/48/1/012025
12. A sodar for profiling in a spatially inhomogeneous urban environment / Bradley S., Barlow J., Lally J., Halois C. // Meteorologische Zeitschrift. 2015. Vol. 24, Issue 6. P. 615–624. doi: 10.1127/metz/2015/0657
13. Underwood K. H., Shamanaeva L. G. Turbulence characteristics from minisodar data // Russian Physics Journal. 2010. Vol. 53, Issue 5. P. 526–532. doi: 10.1007/s11182-010-9453-7
14. Influence of the averaging time on the quality of reconstruction of small-scale wind turbulence characteristics in acoustic sounding / Kapegesheva O. F., Krasnenko N. P., Stafeev P. G., Shamanaeva L. G. // Russian Physics Journal. 2013. Vol. 55, Issue 10. P. 1132–1136. doi: 10.1007/s11182-013-9933-7
15. Parametric acoustic antenna for noise-proof pulse sodar / Ulianov Y. N., Skvortsov V. S., Vetrov V. I., Misailov V. L., Maksimova N. G. // 2013 IX Internatioal Conference on Antenna Theory and Techniques. 2013. doi: 10.1109/icatt.2013.6650760
16. Noise-protected antenna for a pulse acoustic atmospheric sounder / Shifrin Y. S., Ulianov Y. N., Vetrov V. I., Misailov V. L. // 2011 VIII International Conference on Antenna Theory and Techniques. 2011. doi: 10.1109/icatt.2011.6170724
17. Kouznetsov R. D. The multi-frequency sodar with high temporal resolution // Meteorologische Zeitschrift. 2009. Vol. 18, Issue 2. P. 169–173. doi: 10.1127/0941-2948/2009/0373
18. Kurniawan H. D., Suksmono A. B. A compressive-sampling Stepped-Frequency Continuous Wave sodar system // 2016 10th International Conference on Telecommunication Systems Services and Applications (TSSA). 2016. doi: 10.1109/tssa.2016.7871079
19. Akustychnyi prystriy dlia vyznachennia parametriv turbulentnosti v atmosfernomu prykordonnomu shari: Pat. No. 121159 UA. MPK: G01S 13/95, G01W 1/06 / Sheiko S. O., Sidorov H. I., Polonska A. S., Kartashov V. M. No. u201706157; declareted: 19.06.2017; published: 27.11.2017, Bul. No. 22. 6 p.
20. Manual of Aeronautical Meteorological Practice. ICAO: Doc. 8896 AN/893. 9th ed. 2011. URL: https://skybrary.aero/bookshelf/books/2506.pdf
21. Leonidov V. I. Statistical descriptions of the echosignals of acoustic sounding in the area of megalopolis // Eastern-European Journal of Enterprise Technologies. 2012. Vol. 6, Issue 4 (60). P. 46–50. URL: http://journals.uran.ua/eejet/article/view/5683/5113
22. Semenec V. V., Leonidov V. I. Acoustic sounding of atmosphere in the problem of heat exchange processes study in the area of megalopolis // Eastern-European Journal of Enterprise Technologies. 2011. Vol. 6, Issue 8 (54). P. 45–49. URL: http://journals.uran.ua/eejet/article/view/2328/2132
23. Tihonov V. I. Statisticheskaya radiotekhnika. Moscow: Radio i svyaz', 1982. 624 p.